

AD-A172 246

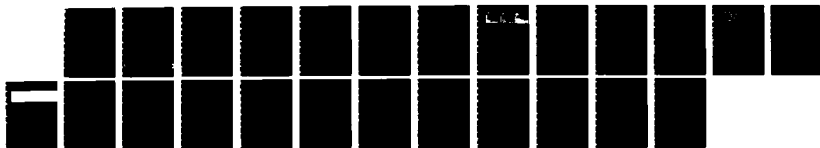
DESICKLING OF SICKLE CELL ERYTHROCYTES BY PULSED RF
FIELDS(U) PENNSYLVANIA UNIV PHILADELPHIA
S TAKASHIMA ET AL 16 SEP 86 N00014-82-K-0321

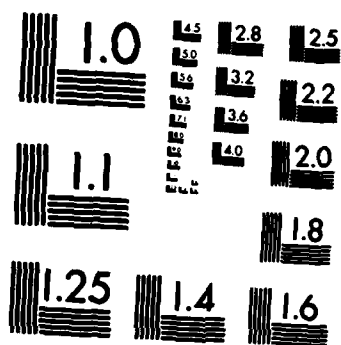
1/1

UNCLASSIFIED

F/G 6/5

NL





MICROCOPY RESOLUTION TEST CHART
NATIONAL BUREAU OF STANDARDS-1963-A

2

SAMPLE FORM

(U)

SECURITY CLASSIFICATION OF THIS PAGE

REPORT DOCUMENTATION PAGE

AD-A172 246

1b. RESTRICTIVE MARKINGS NA	
3. DISTRIBUTION / AVAILABILITY OF REPORT Distribution Unlimited	
4. PERFORMING ORGANIZATION REPORT NUMBER(S) Univ. of Pennsylvania # (if applicable)	
5. MONITORING ORGANIZATION REPORT NUMBER(S) NA	
6a. NAME OF PERFORMING ORGANIZATION Univ. of Pennsylvania	6b. OFFICE SYMBOL (if applicable) NA
7a. NAME OF MONITORING ORGANIZATION Office of Naval Research	
7b. ADDRESS (City, State, and ZIP Code) 800 North Quincy Street Arlington, VA 22217-5000	
8a. NAME OF FUNDING / SPONSORING ORGANIZATION Office of Naval Research	8b. OFFICE SYMBOL (if applicable) ONR
9. PROCUREMENT INSTRUMENT IDENTIFICATION NUMBER N00014-82 - K 0321	
10. SOURCE OF FUNDING NUMBERS	
PROGRAM ELEMENT NO. 61153N	PROJECT NO. RR04108
TASK NO. NR or 441	WORK UNIT ACCESSION NO leave blank
11. TITLE (Include Security Classification) Desickling of Sickle Cell Erythrocytes by Pulsed RF Fields (U) Title of report	
12. PERSONAL AUTHOR(S) Names of authors-see instructions S.Takashima, S.Chang, J.Ashe, A.Hill (Takashima,P.I.)	
13a. TYPE OF REPORT Final	13b. TIME COVERED FROM 6/82 TO 9/86
14. DATE OF REPORT. (Year, Month, Day) Current date 9/16/86	
15. PAGE COUNT 22 # pages in report	
16. SUPPLEMENTARY NOTATION See instructions	
17. COSATI CODES	
FIELD 08	GROUP SUB-GROUP
18. SUBJECT TERMS (Continue on reverse if necessary and identify by block number) Key words - see instructions	
19. ABSTRACT (Continue on reverse if necessary and identify by block number) The purpose of this project is to use electrical pulses as a non-invasive method to desickled SS erythrocytes. We developed an electrical technique to convert sickled red blood cells to normal discoidal erythrocytes. Electrical pulses create small pores in erythrocyte membrane and the fluxes of ions and water are the direct cause to observed shape changes of erythrocytes. The pore formation was confirmed by a patch clamp method as well as AA spectrophotometry. Field induced membrane potential which causes the partial breakdown of the membrane and the formation of pores was calculated theoretically.	
20. DISTRIBUTION / AVAILABILITY OF ABSTRACT <input checked="" type="checkbox"/> UNCLASSIFIED/UNLIMITED <input type="checkbox"/> SAME AS RPT. <input type="checkbox"/> DTIC USERS	
21. ABSTRACT SECURITY CLASSIFICATION (U)	
22a. NAME OF RESPONSIBLE INDIVIDUAL Dr. T. C. Rozzell	
22b. TELEPHONE (Include Area Code) 202/696-4053	
22c. OFFICE SYMBOL ONR	

DTIC FILE COPY

SEP 23 1986
ELECTE
S

Principal Investigator: Shiro Takashima

Assisted by: Stephen Chang
John Ashe
Amanda Hill

Introduction

It is well known that electrical fields have a variety of effects on biological cells. Some of these are 1) Pearl chain formation (Heller,1959,Sher,1963), 2) Cell spinning, 3) Cell fusion (Zimmermann,1974,1982) and 4) Shape and volume changes (Kinosita et al. 1977,1979, Takashima et al. 1983). The purpose of this project is to use electrical fields to change the shape of abnormal human red blood cells,i.e., sickle cell anemia erythrocytes. The shape of those cells is distinctly different from that of normal red cells (see Singer et al.1953). Because of this, the flow of blood in small capillaries is either impeded or even blocked completely. The vaso occlusion of microvasculature is cause of the crisis of sickle cell anemia patients.

There are a number of drugs or chemicals which have been tested in vitro or in vivo in attempts to inhibit the polymerization of intracellular Hb S or to disintegrate Hb S gels by increasing the water flux into red blood cells (see Dean et al. 1978). The effectiveness of these drugs is, however, less than satisfactory.

Our attempt to use electrical fields to desickle abnormal erythrocytes began several years ago (Takashsima et al. 1983). At the beginning, our technique was crude and desickling entailed extensive hemolysis. Nevertheless, we found that pulsed AC fields are very effective in changing the shape of deformed or sickled abnormal erythrocytes. We have improved the technique since

then and presently we are able to achieve the desickling of SS-erythrocytes without noticeable hemolysis (Takashima et al. 1985). In the following, I would like to discuss the results of this project chronologically.

Experimental Set Up

The electrical system which is used for the project is shown in Fig.1. A) Function generator with a saw tooth generator which modulates CW AC fields and generates pulsed wave form. B) ENI 1140LA power amplifier with the maximum output of 1.6 kW. C) Tektronix 5103 storage oscilloscope. D) General Radio 350B attenuator. E) Electrode assembly. The detail of electrode assembly is depicted in Fig.2. The microscope is equipped with a Panasonic TV camera and a monitor.

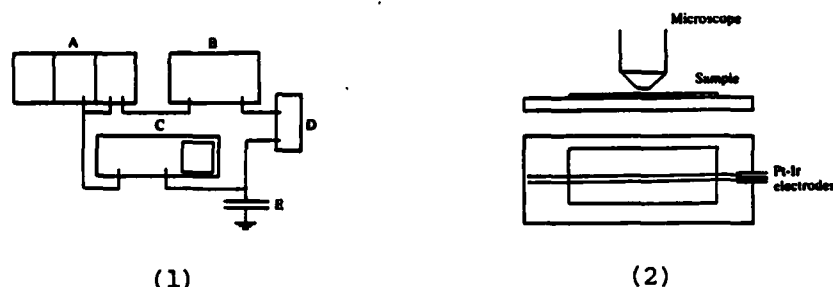


Figure 1 Schematic diagram of electronic system used for the exposure of erythrocytes.

Figure 2 Electrode assembly. Electrodes are Pt-Ir alloy with a diameter of 50 μm . The distance between them is 0.3-0.5 mm.

The procedure we used is to put a small amount of sickle cell erythrocyte suspension and flush with continuous flow of nitrogen for 20-30 minutes to deoxygenate the suspension as much as possible. The suspension contains a small amount of glucose and glucose-oxidase to consume remaining oxygen in solution. Upon deoxygenation of Hb S, a few drops of suspension

are transferred to the electrode assembly and quickly covered with a cover glass. If necessary, the cover glass was sealed using either dental wax or vaseline in order to prevent the penetration of air into the sample.

The electrode assembly is mounted to microscope stage and connected to the output of attenuator. The attenuator turned out to be very useful for stepping up the voltage of applied field in small steps. The shape of erythrocytes is monitored visually on a TV screen continuously while the voltage is stepped up gradually. When the intensity of applied fields reaches the threshold, the shape of erythrocytes begins to change quickly. The rate of shape change depends on the field intensity. Usually, the best result is obtained when the field intensity is slightly above the threshold.

Results

One of the early results we obtained is shown in Fig.3. This

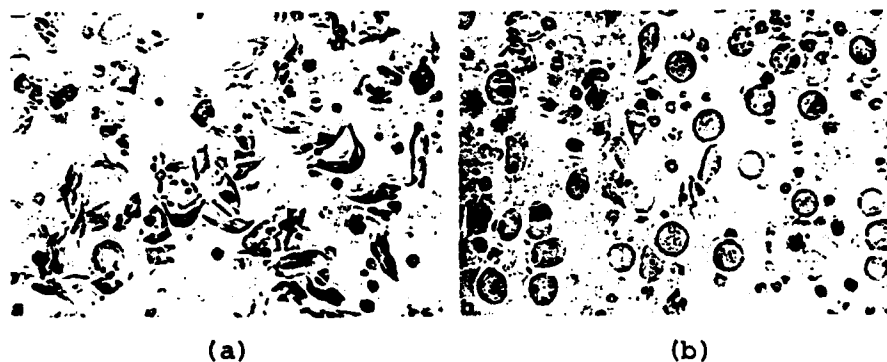


Figure 3. a) Sickled red blood cells before exposure to pulsed fields (x800). b) Shape change in the presence of a field of 100 KHz. the field strength was 3.0kV/cm with a pulse width of 5 msec.

micrograph was obtained with sickled erythrocytes suspended in 0.9% NaCl solution. The width of pulsed field is 5 ms with an interval of 1 sec. Perhaps because of the long pulse we used at the early

stage of this project, usually desickling entailed extensive hemolysis of the desickled erythrocytes.

It is generally agreed that high intensity short pulses achieve desired biological effects with less damage to the membrane than low intensity long pulses (Zimmermann et al. 1981). The variation of pulse widths and subsequent change in the threshold were studied and the result is illustrated in Fig.4. Obviously, the threshold increases as pulse width decreases. In particular, a sharp

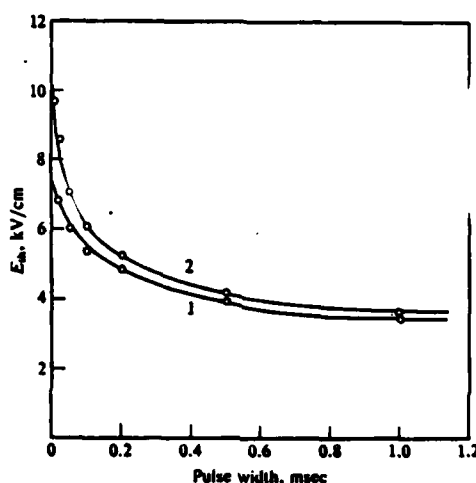


Figure 4. The dependence of the threshold intensity of desickling of SS erythrocytes upon pulse width. Curve 1 and 2 were obtained with 0.9% NaCl solution and Hank's solution as suspending media.

rise is observed below the pulse width of 100 usec. We calculated the power input using the following formula:

$$W = f.V^2/R \quad (1)$$

where f is duty cycle, V is voltage and R is resistivity. Table 1 shows the results of these calculations. It is extremely interesting to observe that the power requirement decreases as pulse width decreases inspite of the increase in threshold intensity. This means that short pulses do not require as much energy as long pulses. This result provides

the evidence to the postulate that short pulses are more effective than long pulses, or more generally put, pulsed fields are more effective than continuous field for causing biological effects.

Table 1

The threshold intensity E_{th} , duty cycle and power input ($E_{th}^2 \times$ duty cycle) of desickling. Carrier frequency: 50KHz.

Pulse Width	E_{th} (V/cm)	Duty Cycle	E_{th}^2
10ms	1950	0.01	38025
5ms	2100	0.005	22050
1ms	2700	0.001	7290
0.5ms	3000	0.0005	4500
100us	3600	0.00001	1296
50us	3900	0.000005	761
20us	4200	0.000002	353

The stability of biological membranes is one of the major concern for membrane biologists. Erythrocyte membrane is known to become unstable in the absence of divalent ions, e.g. Ca. and Mg. Early experiments were performed in physiological saline solution without divalent ions. The photographs shown by Fig.3 are one of the examples. In attempts to reduce the hemolysis, desickling of the SS erythrocyte was performed in Hank's solution which resembles human blood plasma. Fig.5 shows the photographs of sickled and desickled SS erythrocytes which are suspended in Hank's solution. As shown, desickled erythrocytes resemble normal discoidal red blood cells rather than swollen spheriocytes (see Fig.3). Diagram 5C shows the same red cells 30 minutes after desickling. Clearly, hemolysis of desickled cells is minimal. Recent desickling experiments in our laboratory use only one or at most two pulses. With this method, virtually no hemolysis is detected. Thus, we can state with confidence that

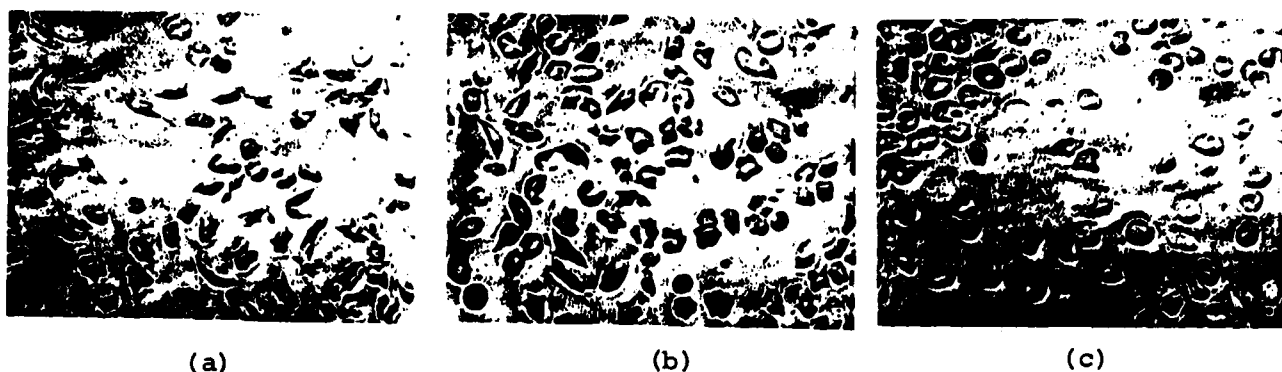


Figure 5. Sickled and desickled SS erythrocytes. a) Before exposure to pulsed fields. b) Onset of desickling. Note the beginning of shape change. c) 30 minutes after desickling. Note only a small number of desickled erythrocytes are hemolyzed. hemolysis of desickled cells is minimal. Recent desickling

electrical fields are able to desickle SS erythrocytes almost reversibly if proper conditions are selected. The threshold of desickling of SS erythrocytes suspended in Hank's solution was determined at each pulse width and the results are illustrated in Fig.4. As shown, the addition of divalent ions seems to increase the threshold slightly although we did not detect substantial elevation of E_{th} .

Measurement of Ion Fluxes by AA Spectrophotometer

The fluxes of Na and K ions through erythrocyte membrane are extremely small under normal circumstances (Lassen et al. 1978, Hunter, 1977). The membrane resistivity is believed to be as high as 10^6 ohms cm^2 . The shape change and swelling of erythrocytes by electrical fields indicate the influx of ions and water through the pores created by electrical fields. We used two techniques to investigate the fluxes of ions before and after exposure of the erythrocyte to electrical fields. The one is AA Spectrophotometer and the other is Patch clamp method. The results obtained with

AA spectrophotometry will be discussed first. We analyzed the change in Na, K, Ca and Cl ions. We would like to discuss only Na and K fluxes in this report (Chang,1985). Fig.6 shows the concentration change of K ions in suspending medium before and after exposure. As shown pre-exposure, sub-threshold exposure and sham exposure do not produce noticeable concentration change of the K ion in suspending medium. Only with supra-threshold exposure to RF, did we observe a large increase in K ion concentration in external solution. This result indicates that intracellular K ion begins to flow out the cell when erythrocyte is exposed to RF of sufficient intensities and small pores are created.

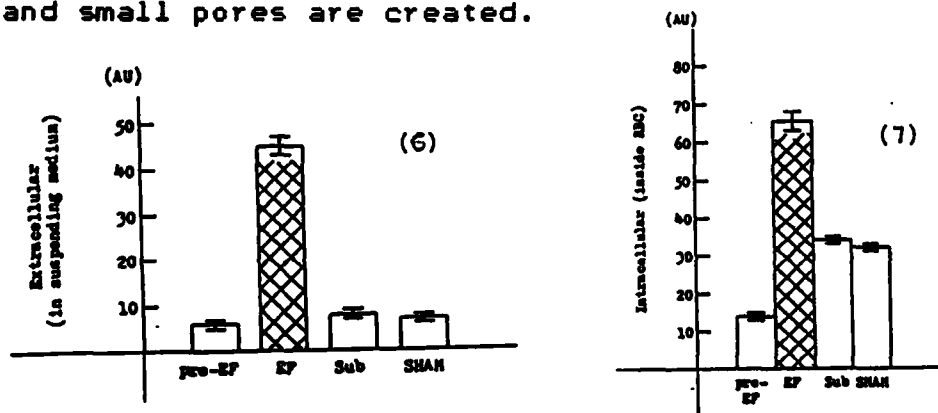


Figure 6. The change in K ion concentration in suspending medium before and after exposure to RF fields. Pre-EF is before exposure Sub is subthreshold exposure, Sham is incubation of the sample without the field. EF is exposure to RF above threshold. The vertical lines indicate standard deviations.

Figure 7. The change in Na ion concentration in erythrocyte. The symbols used in this presentation are the same as Fig.6.

Subsequently, the flux of Na ion was studied. In this experiment, erythrocytes were collected by centrifugation before and after exposure. Pellets were hemolyzed and centrifuged again. The Na content of supernatant was measured using flame photometry. Fig.7 shows the result of these measurements. As shown, the Na ion concentration inside erythrocytes is small

before exposure or with subthreshold exposure. However, only after above threshold exposure, did we observe marked increase in the concentration of Na ion inside red blood cell.

These results clearly indicate that shape and volume changes of erythrocytes are accompanied by fluxes of ions as well as water. Although these results strongly suggest that small pores are created by electrical fields, a more convincing proof can be obtained Patch Clamp Technique.

Patch Clamp Experiment

The cause of the shape change of erythrocytes by electrical pulses has been speculated. The view which is favored by many researchers is that electrical pulses produce a large electrical potential across the membrane (see later section) which in turn causes the partial breakdown of erythrocyte membrane and creates small pores. Using these pores, water and ions flow into or out the cell because of altered osmotic balance. The influx of water through the pores, is therefore the direct cause of volume and shape changes of red blood cells by electrical fields. The proof that pores are created by electrical fields, however, had not been convincing.

The most direct experimental method to prove the existence of pores in the membrane after exposure to an electrical field is Patch Clamp Technique. This technique which was developed by Neher and Sakman (1978,1983) uses a micro-pipette with a tip size of 1 μm , fire polished to make it smooth. The pipette is attached to a cell membrane and, using a suction, establish a tight seal of several giga-ohms. Fig.8 shows the pipette-cell

configuration.

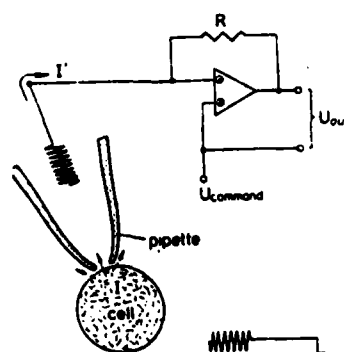


Figure 8. The whole cell configuration of patch clamp pipet with spherical cell.

The patch of the membrane inside the pipette tip can be destroyed by a further suction to create "whole cell configuration". The silver-silver chloridated electrode is enclosed in the pipette and voltage-current relation can be determined. In addition, using the holding potential, we can measure single channel currents of the order of 2-3 pA which occurs sporadically if a small number of channels exist.

The patch clamping with human normal erythrocytes (Grygorczyk et al. 1984) is difficult because of the lack of adhesivity of the membrane. We found that patch clamping with SS erythrocyte difficult inspite of its higher adhesivity. Because of this, it was decided to use frog erythrocytes. Frog erythrocyte is larger in size and much more adhesive to glass pipette. Its ion transport properties is well known and the effect of electrical fields on red cell membranes can be studied easily using this preparation. The photograph of frog erythrocyte is shown in Fig.9.

The transport of K and Na ions through frog erythrocyte is extremely low under normal conditions and the membrane behaves

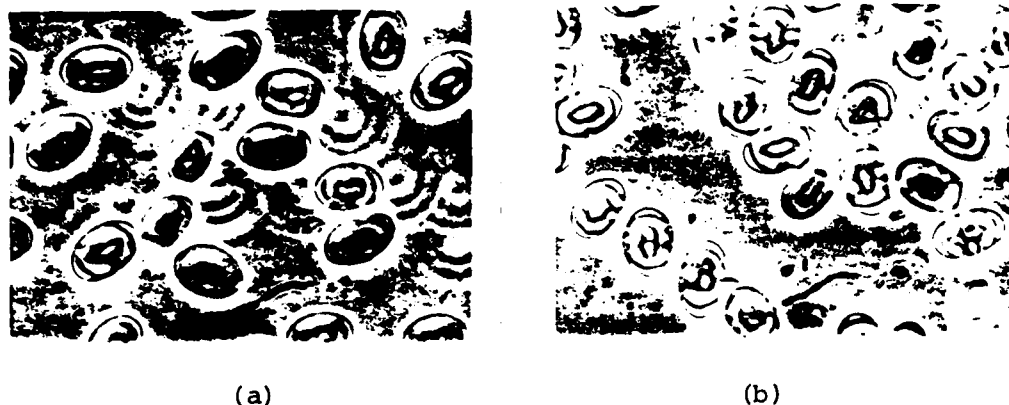


Figure 9. Photograph of frog erythrocytes before (a) and after exposure to electrical pulse (b) $\times 400$.

The transport of K and Na ions through frog erythrocyte is extremely low under normal conditions and the membrane behaves as if it is an insulator (Hamill, 1983). The resistivity of erythrocyte membrane is believed to be about 10^6 ohms cm^2 . This is 1000 times larger than that of, e.g., nerve membrane. Reflecting this fact, the membrane current measured by patch clamp method is extremely small. Fig. 10 shows the current-voltage diagram of frog erythrocyte. The current diagram, however, suggests that some portion of observed current may be due to the leakage through the junction between patch pipet and the membrane. It is well known that this leakage current cannot be eliminated completely no matter how tight the seal would be. Under these circumstances researchers prefer the measurement of single channel currents. the patch clamp amplifiers are capable of imposing a holding potential. That is to adjust the membrane potential at some desired levels. We can fix the holding potential at -70 mV , 0 mV and even $+80 \text{ mV}$ depending upon the purpose of measurements. With a positive holding potential, the potential of inside is higher than that of external medium. Therefore, intracellular K ion will flow out whenever ion channels open. This is called single

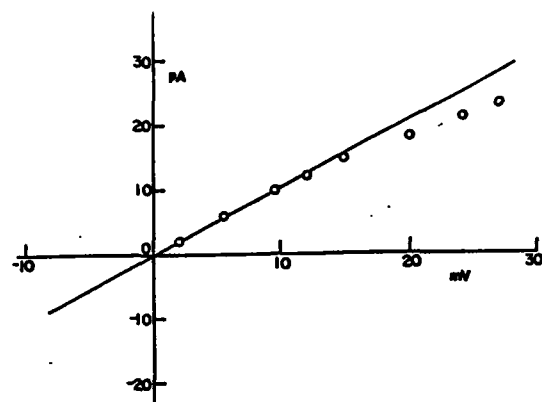


Figure 10. The current-voltage diagram of frog erythrocyte. This diagram represents the gross membrane current.

channel current. With intact erythrocytes, however, single channel current cannot be observed because of the extremely small conductivity of the membrane (see Fig.11a) and channels open only very infrequently.

The way to enhance the efflux of internal potassium ion is to put Ca inside the cell and this is called Gardos's effect (Gardos,1977). The Gardos effect can be induced by treating erythrocytes with 1 mM iodoacetate, 10 mM adenosine and 10 mM CaCl_2 for several hours (Hamill, 1981). After this treatment, the cells are suspended in the normal Ringer solution. Some of the single channel K current are shown in Fig.11b. The holding potential is +80mV. As shown, we observe currents with fairly uniform magnitudes of 2pA or 4pA. The interval and duration of these current bursts are variable which is the typical behavior of channel opening and closing. With these preliminary experiments, we were certain that our equipment and technique are able to measure small single channel currents.

Frog erythrocytes are exposed to pulsed RF fields. In order to avoid excessive exposure, we used only one or at most two pulses of the magnitude of 60V across 0.05 cm. The pulse width

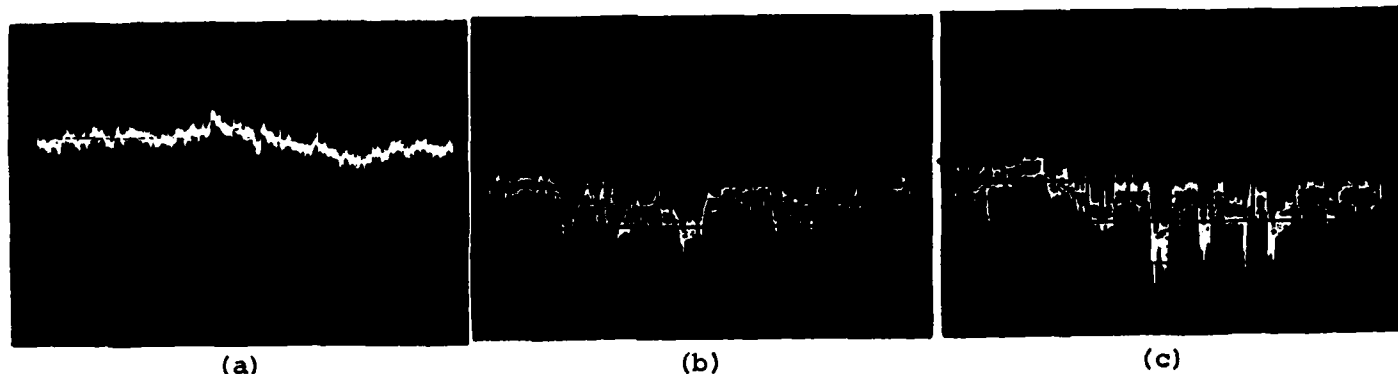


Figure 11. Current trace obtained with frog erythrocyte with a holding potential of +80 mV. a) Before the treatment. Note that no single channel current is observed. b) After treatment with iodoacetate-adenosine which induces Gardos' effect. The magnitude of single channel current is 2pA. Time scale is 500ms/div and voltage scale is 2mV/div. for all of the diagrams. The diagram c) shows another single channel current with two levels, i.e., 2 and 4 pA.

is 0.1 msec. Even with this brief exposure, frog erythrocytes change its appearance slightly as shown by Fig.9. Exposed erythrocytes are transferred to a culture dish which is used for patch clamping. Fig.12a shows the current diagram before exposure and 11b shows the single channel currents after exposure. These

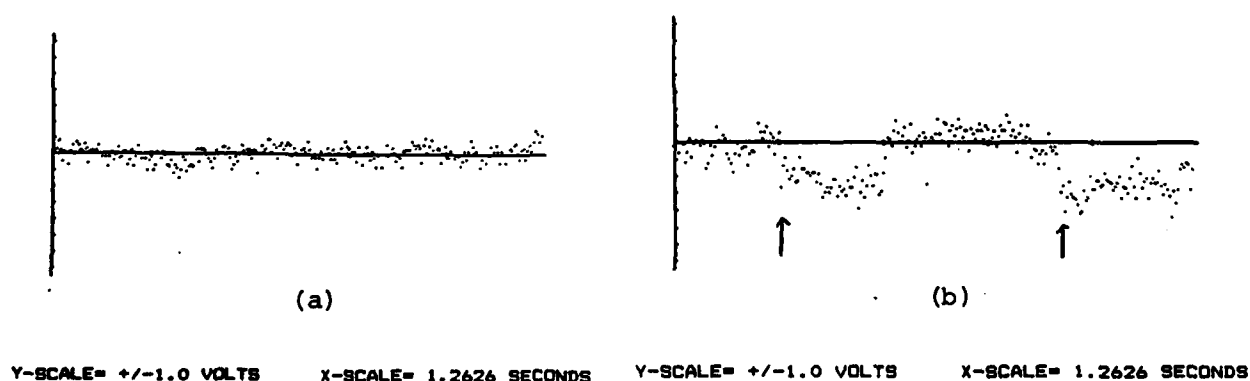


Figure 12. Single channel currents of frog erythrocytes before (a) and after exposure to electrical pulses (b). The full scale of ordinate is 5pA and abscissa is 1.26 sec. Diagram b indicates the presence of single channel current as marked by arrows.

diagrams were obtained using an on-line computer with an analog to digital converter. As shown, the diagrams contain random values. In the future, we are hoping to use digital filtration to clean up the current trace. In spite of the presence of noise, the onset and turning off of single channel currents are clearly seen. The magnitude of current is about 3-4 pA uniformly. This current is slightly larger than those induced by iodoacetate. That means that the pores created by electrical pulses is larger than those produced by chemical means.

Since the holding potential is -80 mV and current is 4×10^{-12} A, we can calculate the resistance of one pore to be 16×10^9 ohms. The resistivity of Ringer solution is about 600 ohms cm, and using the equation $R = \rho (A/d)$ where ρ is the resistivity of Ringer solution, A and d are the area of the pore and thickness of the membrane (100 A). Using this formula, we can calculate the approximate area of the pore created by the field. We obtained a value of 14×10^{-16} cm². The radius of these pores is therefore about 3-4 A. On the other hand, the radius of the pore produced by iodoacetate treatment is 2-3 A. Thus, the pores produced by electrical fields are slightly larger than chemically induced pores. I should be noted that the magnitude of single channel currents is amazingly uniform. This means that the size of pores induced by these methods is always the same or similar.

Electrically induced cell fusion is a very interesting phenomenon to us for some time. Again, there are chemical as well as electrical techniques. It has been believed that electrical method is too harsh causing extensive damages to the

X-SCALE= 1.2626 SECONDS

(b)

view of the importance of cell fusion, this problem must be further investigated in the future.

The cause of the electrical breakdown of erythrocyte membrane is believed to be the induced potential across it by applied fields. Schwan (1983) calculated the field induced membrane

potential for spherical cells and also for cylindrical cells (with a transverse field). They are given by:

$$\begin{aligned} V &= 1.5 RE && \text{for spheres} \\ V &= 1.0 RE && \text{for cylinders} \end{aligned} \tag{2}$$

where R is the radius in cm and E is the field in V/cm. If a field of 2 kV/cm is applied to the suspension of normal erythrocytes, the induced potential is 1.2 V assuming the shape of red cells to be a sphere with a radius of 4 μ m. This potential is sufficient to perforate the membrane and produce a number of small pores. If a field is applied across the long axis of a cylinder, induced potential is dictated by eq.2. The potential calculation for cylinders with longitudinal direction is very difficult and has not been done.

The shape of sickled abnormal erythrocytes is far from spherical. As shown by Fig.3a, sickled erythrocytes are very difficult to simulate accurately with a simple geometry. Under these circumstances, we have to use a model which is amenable to theoretical calculations and yet reasonably realistically represents the shape of sickled erythrocytes. We decided to use prolate ellipsoids of revolution for the potential calculation.

The calculation of induced potential in ellipsoidal cells was performed by Bernhardt and Pauly (1973). The numerical calculation of the potential using their theory is somewhat cumbersome and is not suitable for our purpose. We therefore recalculated, using a similar method used by Klee and Plonsey (1976), the induced potential with a longitudinal as well as transverse fields. Fig.14 shows the model used for this calculation.

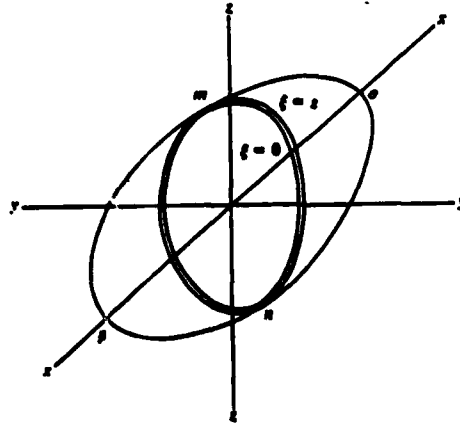


Figure 14. Ellipsoidal model used for the calculation of electrically induced potential. a and b are two axes. X, Y and Z are axes of the cartesian coordinates.

The potential functions induced at the inner and outer surface of an ellipsoid are given by (Stratton, 1941).

$$V_1 = - \frac{E \cdot x}{1 + \left(\frac{abc}{2} \right) \left(\frac{\epsilon_1 - \epsilon_3}{\epsilon_3} \right) A_1} \quad (3)$$

$$V_2 = V_1 \left\{ 1 + \left(\frac{abc}{2} \right) \left(\frac{\epsilon_1 - \epsilon_2}{\epsilon_2} \right) \int_0^S \frac{d\xi}{(\xi + a^2)^{0.5} R_\xi} \right\} \quad (4)$$

where A_1 is an elliptic integral

$$A_1 = \int_0^\infty \frac{d\xi}{(\xi + a^2)^{0.5} R_\xi} \quad (5)$$

Induced membrane potential is defined by

$$\Delta V = V_2 - V_1 \quad (6)$$

The numerical values of induced potential by longitudinal and transverse fields are illustrated in Fig.15 as function of the axial ratio of ellipsoids.

As shown, induced potential increases (with longitudinal fields) and decreases (with transverse fields) as the axial ratio of ellipsoidal cell increases and eventually reaches

a respective limiting values. On the other hand, as the shape of ellipsoids approaches a sphere, the induced potentials converge to the value of about 1.2 V. This value is in agreement with the one calculated by eq.2. If ellipsoidal cells are dis-

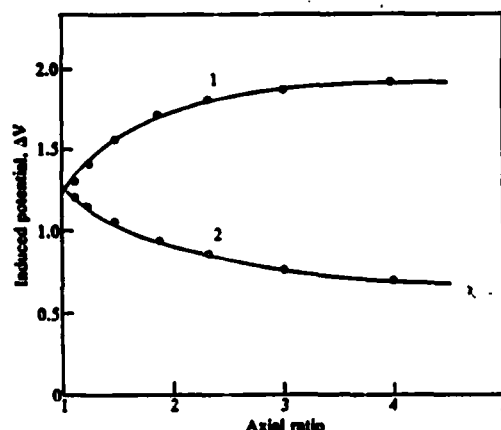


Figure 15. Field induced electrical potential calculated using the model shown in Fig.14. Abscissa is axial ratios and the ordinate is potential in volts. Curve 1 with a field along the major axis and curve 2 with a transverse field.

tributed randomly, the induced potential can be calculated as the average of curves 1 and 2. Therefore, the values calculated by eq.2 are a reasonable approximation to the induced potential in real suspension. In conclusion, the potential which is induced by a field of 2-3 kV/cm is sufficiently large to perforate the membrane and this may be one of the cause of the field induced shape change of erythrocytes.

Maxwell's Stress Tensor Hypothesis

Another interpretation of the shape change is based on the concept of Maxwell's stress tensor (see Panofsky, 1962). In short, applied electrical fields generates mechanical forces according to Maxwell's tensor equation.

$$T_{mn} = \epsilon E_m E_n - \frac{\epsilon}{2} \delta_{mn} E_k E_k$$

where T_{mn} is stress tensor, E_m, E_n and E_k are electrical field intensity, ϵ is dielectric constant and δ_{mn} the kronecker delta. The surface traction S_m is defined by the following formula.

$$S_m = (T_{mn}^a - T_{mn}^b) \cdot n_n$$

where n_n is unit normal vector. Fig.16 illustrates a patch of membrane with surface tractions on both sides.

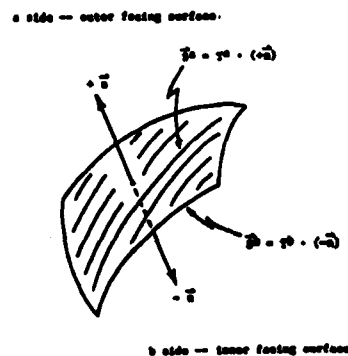


Figure 16. Schematic presentation of a membrane patch with unit normal vectors. S^a and S^b are surface tractions on both sides of membrane.

Table II shows the elements of Maxwell Tensor T_{mn} . The surface tractions S are calculated for inner and outer surfaces and the

Table II

Tabulation of Maxwell's tensor elements T_{mn}

$\begin{matrix} n \\ m \end{matrix}$	1	2	3
1	$E_1^2 - \frac{\epsilon}{2} E^2$	$E_1 E_2$	$E_1 E_3$
2	$E_2 E_1$	$E_2^2 - \frac{\epsilon}{2} E^2$	$E_2 E_3$
3	$E_3 E_1$	$E_3 E_2$	$E_3^2 - \frac{\epsilon}{2} E^2$

net surface forces are computed as the difference between them. Figure 17 shows the net surface force calculated for a spherical particle with a thin shell. The net force is, as shown, directed outward. This means that electrical fields tend to stretch erythrocytes in the direction of the field. The calculation of surface forces are now extended to ellipsoidal particles. Also finite Element calculations of the deformation of erythrocyte is under way in our laboratory.

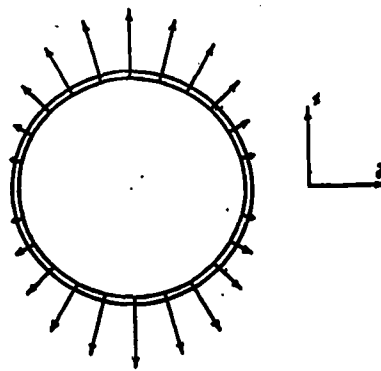


Figure 17. The net surface tractions for spherical particles. A field is applied along the x axis.

References

- Bernhardt, T. and H.Pauly, *Biophysik*, 10, 89 (1973).
- Chang, S.K., *Desickling of Sickled Cells using Electric Fields*, Ph.D. Dissertation, University of Pennsylvania (1985).
- Dean, J. and A.N. Schechter, *the New England Journal of Medicine*, 299, 14, 752 (1978).
- Gardos, G., I. Szasz and B. Sarkadi, *Acta Biol. Med.*, 36, 823 (1977).
- Grygorczyk, R., W.Schwarz and H.Passow, *Biophys. J.*, 45, 693 (1984).
- Hamill, O.P., *J. Physiol.*, 319, 97P (Abstr), (1981).
- Hamill, O.P., In: *Single Channel Recording*, E.Neher and B. Sakmann, Eds., Plenum Press, N.Y. 1983.

- Hunter, M.J., J. Physiol. (London), 268, 35 (1977).
- Kinosita, K. and T.Y. Tsong, Proc. Nat. Acad. Sci., 74, 1923 (1977).
- Kinosita, K. and T.Y. Tsong, Biochim. Biophys. Acta, 554, 479 (1979).
- Klee, M. and R. Plonsey, IEEE Trans. Biomed. Eng., 23, 4, 347 (1976).
- Lassen, U.V., L.Pape and B. Vestergaard-Bogind, J. Membrane Biol., 39, 27 (1978).
- Neher, E., B. Sakmann and J.H. Steinbach, Pfluger's Archiv, 375, 219, 1978.
- Panofsky, W.K.H. and M. Phillips, Classical Electricity and Magnetism, 2nd ed., Chapter 6, Addison-Wesley (1962).
- Sackmann, B. and E. Neher, Single Channel Recording, Plenum Press, New York (1983).
- Schwan, H.P. In: Biological Effects and Dosimetry of Nonionizing radiation, M. Grandorfo, S. Michaelson and A. Rindi, Eds., Plenum Press, N.Y. 1983.
- Sher, L.L., Mechanical Effects of AC Fields on Particles Dispersed in a Liquid. Biological Implications, Ph.D. Dissertation, University of Pennsylvania (1963).
- Singer, K. and L. Singer, The gelling phenomenon of sickle cell hemoglobin: its biological and diagnostic significance. Blood, 8, 10087 (1953).
- Stratton, J.A., Electromagnetic Theory, McGraw-hill. New York, (1941).
- Takashima, S. and T. Asakura, Science, 220, 411 (1983).
- Takashima, S. S. Chang and T. Asakura, Proc. Nat. Acad. Sci. USA, 82, 6860 (1985).
- Teixeira-Pinto, A.A., L.L. Nejeleski, J.L. Cutler and J.H. Heller, Exp. Cell Res., 20, 548 (1960).
- Zimmermann, U., G. Pilwat and R. Riemann, Biophys. J., 14, 881 (1974).
- Zimmermann, U., P. Scheurich, G. Pilwat and R. Benz, Angew. Chemie, 20, 322 (1981).
- Zimmermann, U., Biochim. Biophys. Acta, 694, 227 (1982).

List of Publication

- 1) S.Takashima and T.Asakura, Desickling of sickled Erythrocytes by Pulsed Radio-Frequency Field. Science, 220, 411-413, 1983.
- 2) Z.Delalic, S.Takashima, K.Adachi and T.Asakura, Dielectric Constant of Sickle cell Hemoglobin. Dielectric Properties of Sickled Cell Hemoglobin in solution and Gel. J. Molec. Biol., 168, 659-671, 1983.
- 3) S.Takashima and H.P. Schwan, Alignment of Microscopic Particles in Electric Fields and its Biological Implications. Biophysical J., 47, 513-518, 1985.
- 4) S.Takashima, S.Chang and T.Asakura, Shape change of sickled Erythrocytes induced by Pulsed RF electrical Fields. Proc. Nat. Acad. Sci. U.S.A., vol.82, 6860-6864, 1985.
- 5) S.Takashima, S.Chang and T.Asakura, The Effects of Pulsed RF Fields on the Shape and Volume of Normal and Sickled Erythrocytes. In "Interactions between Electromagnetic Fields and Cells" Eds. A.chabrera, C.Nicolini and H.P. Schwan, Plenum Press, New York, 391-400, 1985.
- 6) S.Chang, S.Takashima and T.Asakura, Volume and Shape Changes of Human Erythrocytes induced by Electrical Fields. J. of Electrochemistry, 4(2), 301-315, 1985.
- 7) T.Asakura, Y.Tanaka, L.M.Lopez, L.Lerner and S.Takashima, Antisickling Effect by Swelling of Red Cells using RF Fields. "Approaches to the therapy of Sickled Cell Anemia, Colloque Inserm, Vol.141, 355-366, 1986.

8) S.Takashima, Molecular Motion of Hb S in Gel. Study of Dipolar Orientation. Pathophysiological Aspects of Sickie Cell Vaso- Occlusion. The Helen Ranney Symposium., In Press.

END

DTIC

10-86